Geophysica (2007), 43(1–2), 25–48

Regional Climate Model Estimates for Changes in Nordic Extreme Events

Lasse Makkonen[1], *Leena Ruokolainen*[2], *Jouni Räisänen*[2] *and Maria Tikanmäki*[1]

[1] VTT Technical Research Centre of Finland, PO Box 1000, 02044 VTT, Finland
[2] Division of Atmospheric Sciences, Department of Physical Sciences, 00014 University of Helsinki, Finland

(Received: August 2007; Accepted: October 2007)

Abstract

Changes in extreme weather events with climate change were estimated for northern Europe by Rossby Centre coupled atmosphere – Baltic Sea regional climate model simulations. Two driving global climate models and two forcing scenarios were used. The estimates were made by comparing, at each grid point, 50-year return values for the simulation periods of 1961–1990 and 2071–2100. The most significant predicted changes in the study area are in the extremes of maximum and minimum air temperatures. The increase in the extreme surface wind speed is mostly small. The 50-year return value for the precipitation amount in five days is predicted to increase by over 50% in many areas. The extreme snow water equivalent is predicted to decrease very significantly in most of the study area but increase in some highland areas. Very heavy snow fall will become generally more frequent. From the point of view of adapting structural design and community planning to climate change, the results suggest that the emphasis should be in the design practices in regard to flooding. The estimated changes in other structural design criteria are generally less significant or favourable.

Key words: Climate change, extreme weather, regional climate modeling, adaptation to climate change, risk management of structures, probabilistic design

1. Introduction

The ongoing anthropogenic increase in atmospheric greenhouse gas concentrations is likely to lead to a substantial change in the global climate in this century. In its Third Assessment Report, the Intergovernmental Panel of Climate Change (IPCC) projected a 1.4–5.8 °C increase in the global mean temperature from 1990 to 2100, depending on the sensitivity of the climate system and on the magnitude of future greenhouse gas emissions (*Cubasch et al*. 2001). In the Fourth IPCC Assessment Report the corresponding range for the 21th century is projected to be 1.1–6.4 °C (*Solomon et al*., 2007). In high-latitude areas, such as the Nordic countries, where changes in snow and ice cover tend to amplify temperature changes, the warming is likely to exceed the global average particularly in winter (e.g. *Räisänen,* 2001, *Jylhä et al.*, 2004). Along with the general warming, other aspects of climate such as precipitation, windiness and snow conditions are likely to change.

Not only the average conditions but also the extremes of climate will be affected (e.g. *Meehl et al.*, 2000, *Huntingford et al*., 2003, *Ekström et al*., 2005, *Kharin and Zwiers*, 2005). Increases in atmospheric water vapour are likely to lead to generally more intense short-term precipitation extremes, even in many areas that experience a decrease in average precipitation (e.g. *Frei et al*., 2006, *Pall et al*., 2007). The projected overall warming is also expected to be accompanied by more severe warm extremes and less severe cold extremes, but the changes in the extremes may differ quantitatively from the changes in mean temperature. For example, many studies have suggested an unproportionally large increase in the lowest winter temperatures in mid- to high-latitude areas, at least partly as a response to reduced snow and ice cover (e.g. *Hegerl et al*., 2004, *Kjellström et al*., 2007). There are also indications of increased temperature variability in mid-latitude continental areas such as central Europe in summer, leading to a larger increase in the highest than in the average summer temperatures (e.g. *Kjellström et al.,* 2007), and this may, in fact, be a contributing factor to the central European heat wave in summer 2003 (*Schär et al*., 2004). For changes in extreme wind speeds, the evidence from modelling studies appears more mixed. For example, although several studies have suggested stronger wind extremes in central and/or northern Europe (e.g. *Leckebusch and Ulbrich*, 2004, *Pryor et al.,* 2005a) some studies point to the opposite direction (e.g. *Pryor et al*., 2005b). As noted among others by *Räisänen et al*. (2004), changes in wind speeds are strongly sensitive to changes in the large-scale atmospheric circulation.

With regard to future changes in extremes, Europe is better posed research-wise than most other parts of the world because of an intense activity in regional climate modelling, which allows climate changes to be addressed at a higher resolution than studies with global climate models. In particular, the PRUDENCE (Prediction of Regional scenarios and Uncertainties for Defining EuropeaN Climate change risks and Effects) project (*Christensen et al.,* 2007) involved simulations of future climate change with ten RCMs, and the analysis of these simulations has included several studies focusing of extremes (*Beniston et al*., 2007, *Frei et al*., 2006, *Kjellström et al*., 2007, *Rockel and Woth*, 2007). However, most of this analysis was made for RCM simulations driven by a single global climate model (GCM), HadAM3H (*Gordon et al.,* 2000), which implies that the RCM results are far from independent. In addition, some of the studies focused on southern and central Europe, covering northern Europe only up to southern Scandinavia. Finally, they mostly focused on relatively mild extremes, such as, for example, the 99th percentile of daily mean wind speed in *Rockel and Woth* (2007).

Here we study changes in weather extremes in northern Europe using a set of four RCM simulations made by the Rossby Centre coupled atmosphere-Baltic Sea regional climate model RCAO (*Räisänen et al*., 2003, 2004). We use RCAO simulations driven by two different GCMs, HadAM3H and ECHAM4/OPYC3, which allows us to also explore some of the GCM-related uncertainty in our findings. For adapting structural design and community planning to the future climate, the changes in the extremes need to be quantified in those statistical terms that allow prudent risk analysis and correspond

to the methods used in civil engineering. This requires a probabilistic approach that involves determining the 50-year return values of the weather variables that are relevant to structural design (e.g. *Castillo*, 1988, *Jordaan*, 2005). Such design values, used as the input for the design processes, are given in the building codes and regulations, such as the Eurocode (*Anon*, 2001). The quantitative question regarding the need to adapt is then: How much should one change these design values because of the projected climate change?

It is noteworthy that the present design values that are applied in construction projects are based on analysis of weather data which date many decades back. Reliance on such historical data is in itself a source of error if the climate change is fast. Furthermore, today's building codes control the safety level of the infrastructure that will be built for the future. A typical design life time of a building is from 50 to 100 years and the plans of land use usually have a time perspective much longer than this. Thus, the extreme events that will likely occur during 110 years, as considered in this paper, are urgently required for the regulations that control construction and land use. Actions to update them in view of the climate change should be taken immediately, but the required data have been missing.

In this paper, changes in the 50-year return values of weather parameters from 1961–1990 to 2071–2100 are estimated for a sub-domain (Nordic countries) of the RCAO model. As a regional climate model with a horizontal resolution of 49 km, RCAO has a potential advantage over coarser-resolution global climate models. Its finer grid allows better resolving both the complicated regional geography that affects the climate in Nordic countries (the Scandinavian mountains, the Baltic Sea, large inland lakes etc.) and the details of individual weather systems. The same four RCAO climate change simulations as analysed by *Räisänen et al.* (2004) are used here, as discussed in Section 2. For the statistical analysis a method extending from *Makkonen* (2006, 2007, 2008) is used to determine the 50-year return values from the data of the annual maxima for the simulated 30-year periods.

2. Climate model simulations

2.1 Global models

Data from two global climate models, HadAM3H and ECHAM4/OPYC3, were used to drive the regional climate model RCAO. HadAM3H is a high resolution (1.875° longitude x 1.25° latitude) atmosphere model (*Gordon et al*., 2000) for which the sea surface temperature and sea ice conditions were derived from observations and earlier lower-resolution coupled atmosphere-ocean simulations, as explained by *Räisänen et al*. (2004). ECHAM4/OPYC3 is a coupled atmosphere-ocean model with a resolution equivalent to a grid spacing of 2.8° longitude x 2.8° latitude (*Roeckner et al*., 1999).

The global climate models were first run from 1860 to 1990 using observed or estimated changes in the atmospheric composition. From 1990 on, the calculation was continued as two separate simulations using different scenarios of anthropogenic

greenhouse gas and sulphur emissions, IPCC SRES A2 and B2 (*Nakićenović et al*., 2000). Both the greenhouse gas and sulphur emissions are larger for A2 than B2, but the difference in greenhouse gas emissions dominates. Thus, the simulated global warming and the general magnitude of other climate changes in the late 21st century are larger for the A2 than the B2 scenario.

For driving the regional climate model, 30-year periods from both the HadAM3H and ECHAM4/OPYC3 simulations, the "control run" (September 1960 to December 1990) and the "scenario run" (September 2070 to December 2100) were used. The 30-year annual global mean warming predicted by HadAM3H from 1961–1990 to 2071–2100 is 3.2 °C in scenario A2 and 2.3 °C in scenario B2. The corresponding warming predicted by ECHAM4/OPYC3 is 3.4 °C for A2 and 2.6 °C for B2. These values are in the midrange of the uncertainty interval reported by *Cubasch et al*. (2001). Taking into account a wider range of emission scenarios and model-specific climate sensitivities, they computed a global warming of 1.5–5 °C from 1975 to 2085.

2.2 The regional model

The Rossby Centre coupled regional climate model RCAO consists of the atmospheric model RCA2 (*Bringfelt et al*., 2001) and the Baltic Sea model RCO (*Meier et al*., 1999, *Meier*, 2001). The atmospheric model RCA2 originates from version 2.5 of the HIRLAM model (*Eerola et al*., 1997), but includes many new parameterizations and other changes as explained in *Räisänen et al*. (2004) and *Jones et al*. (2004). RCA2 was run in a rotated longitude-latitude grid with a 0.44° (approximately 49 km) resolution in both horizontal directions and with 24 levels in the vertical. The integration domain of RCAO covers an area of 106 × 102 grid squares (see *Räisänen et al*., 2004) but the area considered in this study consists of 40 × 40 grid squares only, covering the Nordic countries (see Figs. 4 to 7).

The Baltic Sea model RCO was run with the horizontal resolution of 11 km and with 41 levels in the vertical (see *Meier*, 2001). The coupling procedure between RCA2 and RCO is described in *Döscher et al*. (2002).

In the following, the HadAM3H-driven RCAO simulations will be denoted as RH and the ECHAM4/OPYC3-driven simulations as RE. The control runs for 1961–1990 are denoted by C, the scenario runs for 2071–2100 with the A2 scenario by A2, and the scenario runs with the B2 scenario by B2. Accordingly, the data from the six RCAO simulations used here are denoted as RHC, RHA2, RHB2, REC, REA2 and REB2.

3. Statistical analysis

3.1 Aspects of the extreme value analysis

In most design standards and other engineering codes, as well in hydrological and meteorological literature the measure of the expected frequency of rare events is the return period R (in years). Typically, in standards, the 50-year return value x^{50} is utilized (e.g. *Anon*, 2001). This is the value of the variable x that is exceeded by an

annual maximum once in 50 years in the mean. The return period R of an event is related to the probability P of not exceeding this event in one year by

$$R = \frac{1}{1-P} \tag{1}$$

Hence, the 50-year return period corresponds to the annual probability of exceedance of 0.02. Determining R for some value of x or, vice versa, the return value x^{50} from measured or simulated climate data requires statistical analysis of the cumulative distribution function F(x) of the extremes. In this, the extreme value theory (*Fisher and Tippett*, 1928, *Gumbel*, 1958) has been commonly utilized. The advantage of the extreme value theory is that, ideally, the original parent distribution and its cumulative distribution function need not to be known, because the distribution of the extremes asymptotically approaches a known distribution. In the case of annual extremes, considered in this paper, this distribution is the generalized extreme value distribution GEV

$$F(x) = \exp\left[-\left(1+\gamma(x-\mu)/\alpha\right)^{-1/\gamma}\right] \tag{2}$$

where $\alpha > 0$ and $1 + \gamma(x-\mu)/\alpha > 0$. GEV is a three parameter distribution, the limiting value of which at $\gamma = 0$ is the Gumbel distribution

$$F(x) = \exp(-\exp(-y)) \tag{3}$$

where y is the reduced variate

$$y = (x-\mu)/\alpha \tag{4}$$

Here μ is the location parameter and α is the scale parameter. The GEV distribution has a finite upper tail for the shape parameter $\gamma < 0$ (Weibull), whereas for $\gamma > 0$ (Frechet) and $\gamma = 0$ (Gumbel) there is no upper bound. Here, we consider annual extremes, as discussed above. Similar asymptotic equations can be used for analysing extremes that exceed a certain threshold (*Pickands*, 1975, *Wang*, 1991, *Simiu and Heckert*, 1996, *Brabson and Palutikof*, 2000).

In the classical extreme value analysis method the Gumbel distribution (Eq. (3)) is utilized and the cumulative distribution value P = F(x) of n number of annual maxima is estimated from the order statistics so that each maxima is assigned a rank i in ascending value $1 \le i \le n$. For any analysis of the order ranked extremes one needs to relate each of them to some probability. This is done here by the formula used by *Gumbel* (1958) in his original method, i.e.

$$F(x_i) = i/(n+1) \tag{5}$$

Several other formulas and numerical methods for these "plotting positions" have also been proposed and widely used (*Hazen*, 1914, *Gringorten*, 1963, *Harris*, 1996,

1999, 2000, *Folland and Anderson*, 2002). A significant problem related to this has been that the plotting positions have generally been supposed to depend on the cumulative distribution function (*Gringorten*, 1963, *Cunnane*, 1978, *Harris*, 1996). *Makkonen* (2006, 2008), however, showed that such a supposition is incorrect and that the only correct plotting position when estimating return periods is that given by Eq. (5) for any distribution of extremes.

The fit to estimate the parameters μ and α is traditionally performed on a Gumbel probability graph where the ordinate is the reduced variate from the estimated F(x) in Eq. (3), plotted as $y = -\ln(-\ln(F(x)))$ and the abscissa is the variate value x. This plot transforms the Gumbel distribution model in Eq. (3) into a line with a slope of $1/\alpha$ and intercept μ, as shown in Eq. (4).

There are a number of ways to fit a distribution to the plotted data. In addition to the simple method of least squares, methods that weigh each extreme according to its theoretical statistical confidence have been proposed (*Lieblein*, 1974, *Landwehr et al.,* 1979, *Hosking*, 1985, *Hosking et al*., 1985, *Wang*, 1991, see also *Katz et al*., 2002). In addition to the different statistical confidence of different ranks, the problem with weighing them is related to the possibility that the highest extremes may not belong to the same population as the more moderate extremes (*Gomes and Vickery*, 1978).

Once the fit is made and the parameters α and μ are determined, one can calculate x that corresponds to any probability $F(x) = P$ from Eqs. (3) and (4) and the corresponding return period T from Eq. (1). Often, one will need to estimate extreme values of x that are higher than those included in the data. Graphically this corresponds to extrapolation along the fit on the graph. In this study such an extrapolation is made from the 30-year simulation data to the 50-year return value.

The background for using the Gumbel method is in the theory of extremes, which implies that an unbounded cumulative distribution function of the annual extremes is Eq. (3). This has often been taken too literally in spite of many words of warning (*Gumbel*, 1958, *Cook*, 1982, *Galambos and Macri*, 1999, *Makkonen*, 2007). The theory only shows that the distribution of extremes asymptotically approaches the theoretical extreme value distribution when the number N of independent observations in each observation period from which the extreme is abstracted increases.

The rate of convergence with increasing N towards the theoretical extreme value distribution depends on the parent distribution. For some parent distributions the distribution of extremes is quite far from the Gumbel distribution even when N is 10 000 (*Cook*, 1982). In our climate model simulations at a six-hour interval each year includes N = 1460 observations. Furthermore, the number of independent observations that determine the annual extremes is much smaller because many extremes occur in only specific parts of the year and almost all weather parameters have autocorrelation memory longer than the output interval of our climate model, i.e., six hours. As an example, there are less than 100 “independent storms” in a year (*Cook*, 1982). A good example of both problems is the annual maximum snow amount, which occurs in late winter and is a unique result of gradual snow accumulation during the preceding months. In such a case the assumption of the asymptotic behaviour is unjustified.

Acknowledging that the two-parameter Gumbel distribution may not always be a good model of the extremes, similar fitting methods may be applied to estimating the three parameters of a GEV distribution as well. If then the data show that the shape parameter $\gamma \neq 0$, a linear model is poor and, on a Gumbel plot, the order ranked points form a curve that is concave up or concave down depending on the sign of γ. When the data show $\gamma < 0$, this has often been interpreted to indicate that the tail of the cumulative distribution function is bounded. However, as discussed above, and previously by *Galambos and Macri* (1999), *Cook et al*. (2003), *Harris* (2004) and *Makkonen* (2007), this interpretation is incorrect when N is small, and the points may be nonlinearly positioned on a Gumbel plot also for an unbounded distribution.

3.2 The applied extreme value analysis method

We deal with the fitting problem in this paper as follows. We use GEV, but not for reasons related to the extreme value theory. We simply use GEV to make a convenient empirical three-parameter fit to the simulated order ranked annual extremes. Since our method aims at an empirical fit, all three parameters of GEV are allowed to vary freely at every grid point and for all the simulations. This method is in harmony with the finding by *Kharin and Zwiers* (2005) that locally the shape parameter γ also changes with time in regions where land and sea surface properties change dramatically under global warming. This is indeed the case within our RCAO model domain of the Nordic countries due to the declining extent of seasonal sea ice and snow cover.

In our statistical analysis, we use Eq. (5), i.e., "the empirical distribution function" (*Coles*, 2001, *Makkonen*, 2008), in associating a probability to the order ranked extremes i = 1, 2, ...n. Since Eq. (5) is the correct plotting formula for any distribution (*Makkonen*, 2006, 2008), its use is in harmony with our philosophy, which adopts no a priori assumption of the parent distribution.

In fitting the GEV to the order ranked extremes from the 30-year simulations we use the 15 biggest annual extremes of x only. In the plots in Figs. 1 to 3 the 15 points used in the fit are shown as dots and the rest 15 smaller extremes are shown as circles. The selection of the number of biggest extremes used in the fitting is subjective and comparable to the problem of selecting the threshold in the peaks-over-threshold method that utilizes the Generalized Pareto Distribution (*Brabson and Palutikof*, 2000). The choice may be based on the degree of prior belief on some specific CDF or on the view that the highest extremes belong to the same population, i.e. understanding the physics of the phenomenon. Moreover the implications of the data themselves, i.e. on how much the highest extremes appear to deviate from the rest of the population, may be considered. In the absence of such arguments that could be generalized to our data it was considered here that 15 extremes is a sufficient number that allows reasonable fitting of a three parameter GEV while, on the other hand, limiting the analysis to those extremes that are most relevant to extrapolating to the desired 50 year return value.

There is some controversy related to the conventional fitting methods (*Katz et al*., 2002). For example, the performance of the maximum likelihood method for the GEV

distribution may be erratic for samples as small as here (*Martins and Stedinger*, 2000) and the method of probability weighed moments is not optimal for the Gumbel-distributed samples (*Rasmussen and Gautam*, 2003). Our method deviates from these methods, in which the error is minimized with respect to the probability P = F(x), as we minimize the error between the fitted GEV and the data points with respect to the variable value x. We do this because P is not a variable (*Makkonen*, 2008) and because we specifically wish to estimate, at each grid point, the variable value of x that occurs once in 50 years in the mean, denoted here by x^{50}. Since x^{50} is our end result and is, in practical applications, dealt with as an additive variable, we use the standard least squares method in making the fit to GEV.

The analysis for the annual extremes extracted from the RCAO simulation data is made without additional data control, except the following. The analysis was made only under the condition that out of the 30 simulated annual extremes at least 20 extremes have a value $x_i > x_n/50$. Thus, when in any plot more than 10 extremes are very small, e.g. zero in the case of snow amount, no return value was calculated. This procedure eliminates estimating return values from discontinuous extreme value distributions and from too small number of annual extremes. In such cases the change in the variable value at the grid square in question is white on our maps.

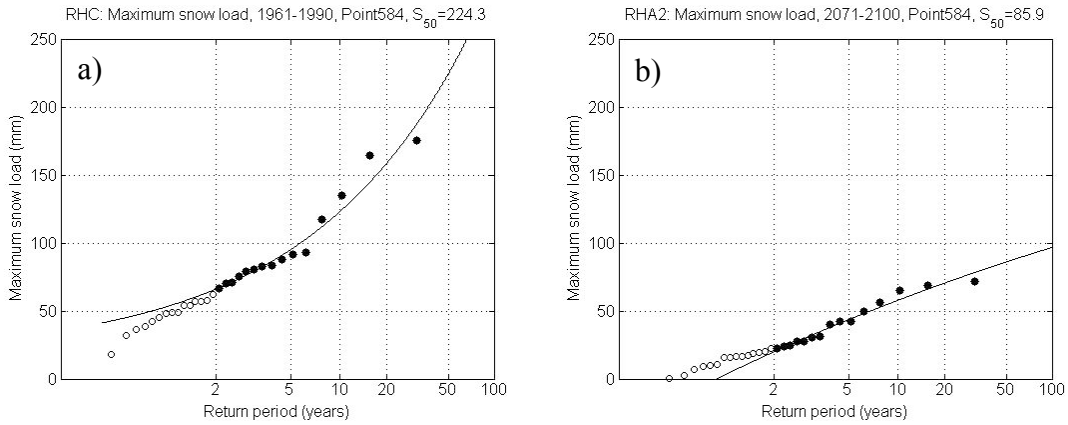

Fig. 1. Example of a probability plot for the extremes of the annual maximum snow water equivalent in the control run RHC (a) and in the scenario run RHA2 (b).

Figure 1 shows a typical example of the resulting probability plot for the annual maximum snow amount. The very significant reduction from Fig. 1a to Fig. 1b is due to a drop of the extremes overall, but also due to disappearance of very large snow extremes. In the framework of Eq. (2) this means that, not only α and μ, but also the shape parameter γ changes with time. An untypical example for another grid point in Fig. 2, which is for six hour precipitation, shows a very different behaviour. Here, there is hardly any apparent change in the bulk of the extremes data but a single very big extreme, a heavy shower of almost 50 mm, causes the extrapolated 50-year return value x^{50} to increase from 20 to 130 mm. This is very exceptional, however. In most cases in

our analysis the shape parameter γ is either close to zero, or the result of the analysis is not much affected by the very biggest extremes even when γ is non-zero. A typical example of the former can be seen in Fig. 3a and 3b for surface wind. Comparing Figs. 3b and 3c, on the other hand, demonstrates a case of different simulation results by using the two different emission scenarios A2 and B2.

In the light of the example in Fig. 2b, one may ask whether one should in the analysis give any weight to the very biggest extreme x_n. Such points are often referred to as "outliers" in the literature. The general practice to give little weight to the outliers in the extreme value analysis is due to the high likelihood that the highest value "represents" a maximum of a period longer than the one from which the sample originates. For example, if x_n was neglected and the remaining 14 big extremes were used in Fig. 2b to make a fit, and that model was extrapolated to estimate long return periods, then x_n would correspond to a roughly 100 000-year return period.

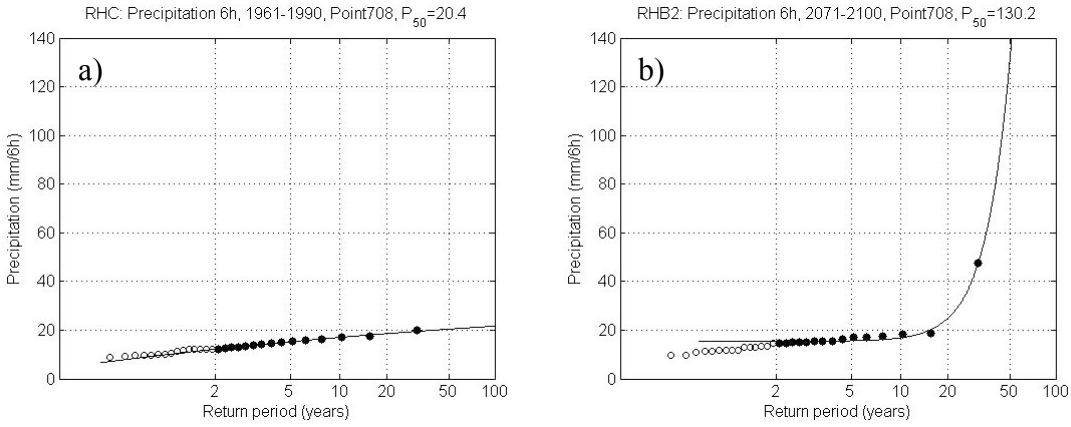

Fig. 2. Example of a probability plot for the annual extremes of the precipitation amount in six hours in the control run RHC (a) and in the scenario run RHB2 (b). This example shows a rare case of a very exceptional largest value in the scenario run (see text).

Considering Eq. (1), the probability of a 100 000-year return value to be exceeded in a 30 year period is $1-(1-1/100000)^{30} = 3*10^{-4}$. This small probability seemingly supports treating the outliers as random errors and neglecting them. Here, however, we must consider the following. Our RCAO model produces for each variable 1600 plots, such as those in Figs. 1 to 3. Suppose now, for exercise, that these plots were statistically independent of each other. Then, taking into account that the grid point values on each of our maps (Fig. 4–7) are results of two plots, the probability of exceeding a 100000-year return value in at least one of the plots is $1-(1-1/100000)^{(2*30*1600)} = 0.62$. The data are not statistically independent, so that this exercise overestimates the probability. Nevertheless, it suffices to demonstrate that, within a large area, extremely rare local extreme events are to be expected locally somewhere.

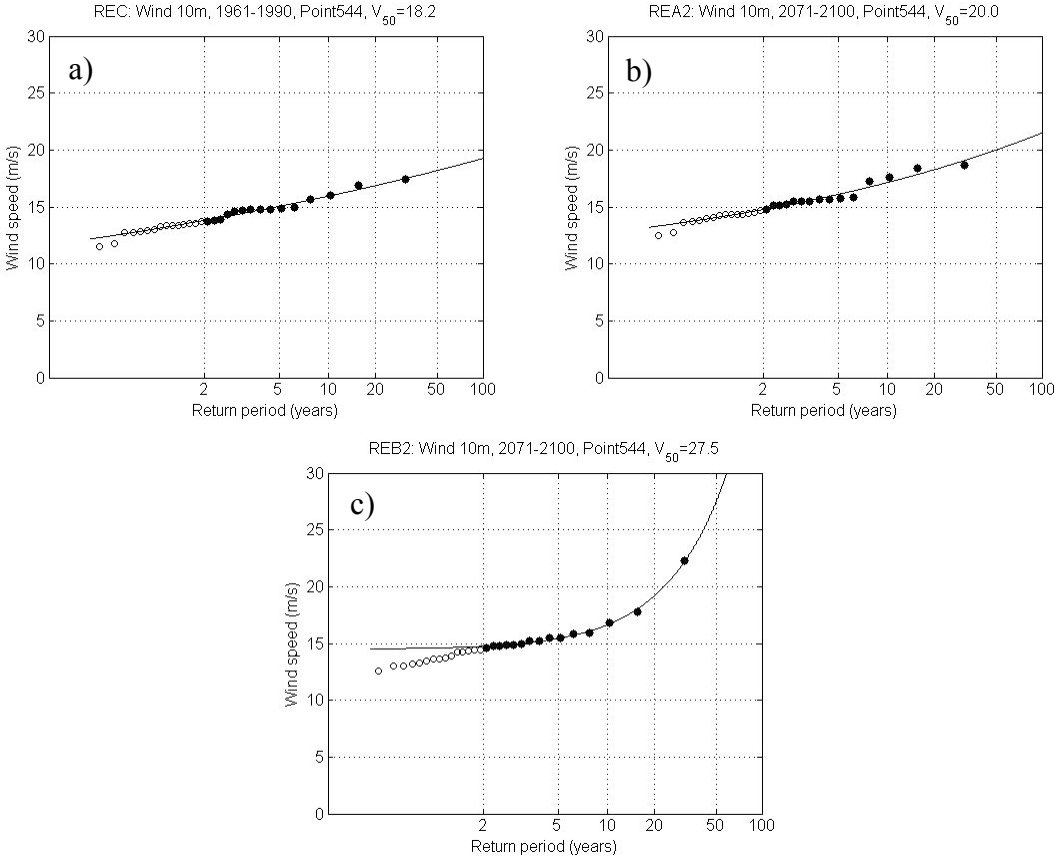

Fig. 3. Example of a probability plot for the annual extremes of the 10 minute mean winds speed at 10 m height in the control run REC (a), in the scenario run REA2 (b) and in the scenario run REB2 (c).

It follows from the above that in our produced maps very high changes occur at some grid points due to natural random variation in the occurrence of the biggest extreme events. Neglecting them as "outliers" at the individual grid points would, therefore, be in contradiction with a statistical fact. It would also remove them from the total model domain and would thus distort its regional extremes. Furthermore, there is a theoretical possibility that some outliers are not caused by random variation only, but are manifestations of such new mechanisms of the future climate that allow much higher magnitude of meteorological variables than the present climate. To miss detecting such cases would have unfortunate consequences in practical applications related to e.g. structural design and safety.

One alternative to neglecting the outliers would be to analyse pooled extremes of larger regions (*Peterka*, 1992). However, our aim in this paper points to the opposite. We wish to utilize a regional climate model in an attempt to better understand changes in the local climates and the importance of local geography, sea, ice and snow areas on them. It would also be very difficult to pool grid points objectively and simultaneously avoid pooling fundamentally different geographical areas (land vs. sea etc.).

Because of what is discussed above, we apply no spatial smoothing and treat the "outliers" as any other points giving them the full weight in this analysis. The

inconvenient but inevitable cost of this is that our resulting maps, which present the estimates of the change in the 50-year return values with climate change, are rather noisy. In the absence of suitable spatial smoothing procedures, we make use of our four different scenario vs. control simulation comparisons by combining their results into one map. We do this by taking, at each grid square, an average of the values in the change of the return value x^{50} resulting from the two different global climate models and two emission scenarios. This averaging procedure provides an "overall" prediction of the change in the 50-year return values with climate change. A simple justification for such an overall prediction is that there is no objective way to say which global climate model is better than the other or which emission scenario is most likely to become true. Yet, an estimate of the future change is required for practical purposes. In the graphical presentation in Figs. 4–7, some additional spatial smoothing is provided by a coarse grey-scale.

In Figs. 4–7, the grid points where all the four simulation comparisons show an increase are marked by ˆ those where all the four simulation comparisons show a decrease are marked by ˇ. No mark at a grid point indicates that at least one of the four results for the direction of change disagrees with the others. The marks thus give an indication of the significance of the predicted change.

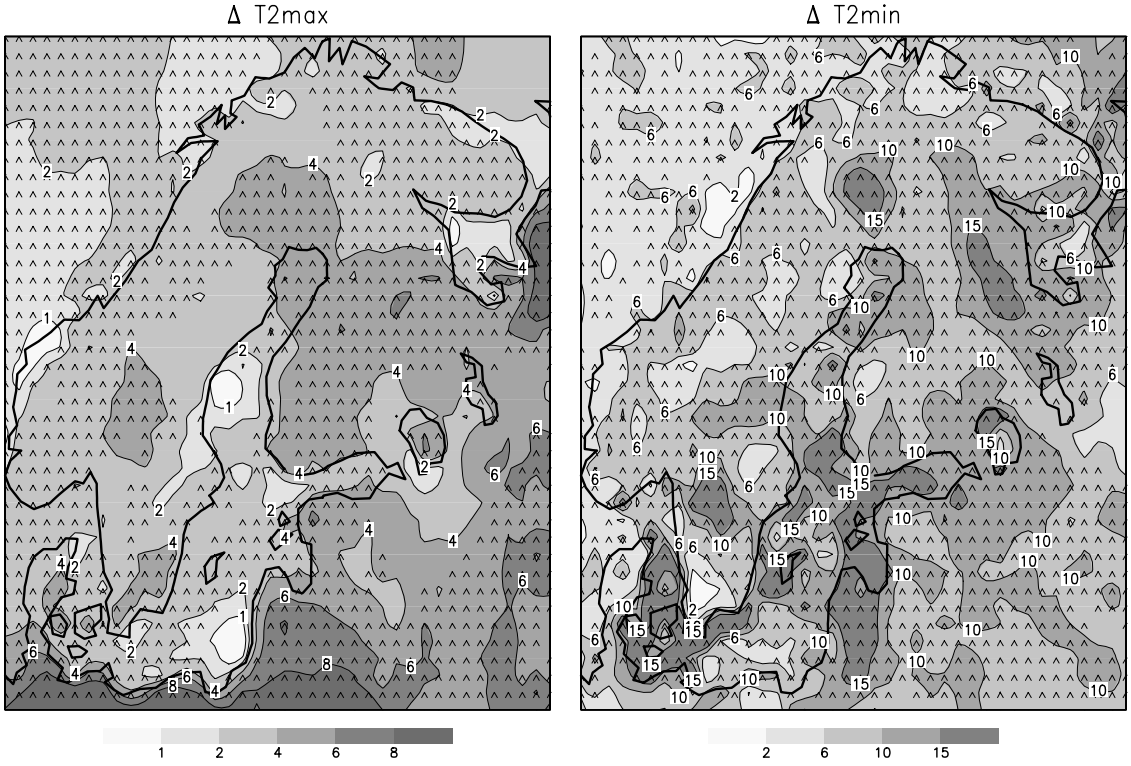

Fig. 4. Simulated changes from 1961 - 1990 to 2071 - 2100 in the 50-year return values of maximum (left) and minimum (right) air temperature at 2m height (in °C). The value for each grid square is calculated as the mean of four RCAO simulation comparisons: using two global climate models RE and RH and two emission scenarios A2 and B2 (see text). The grid points where the four simulation comparisons all show an increase are marked by ˆ and those where they all show a decrease are marked by ˇ.

4. Results

4.1 Mapping the change in the 50 year return values

The results for the change in x^{50}, i.e., the 50-year return value are shown in Fig. 4 for the maximum and minimum air temperature. Both the extreme maximum and minimum temperatures increase in almost the whole area. In general, the change in the latter is larger than that in the former (note the difference in the gray-scales between the two panels). Particularly large warming in the extreme minimum temperature, locally up to 20 °C, occurs over the southern parts of the Baltic Sea and some inland lakes. In these areas very low temperatures are eliminated in the scenario simulations, because the ice-cover becomes more or less non-existent. On the other hand, the largest increases in 50-year return maximum temperature (5–8 °C) occur over land, particularly in the southern and eastern parts of the model domain. The simulations show a large increase in the summer temperatures over central Europe, which is associated with reduced cloudiness and drying out of the soil (*Räisänen et al*., 2003, 2004). In some summers, hot air from the European mainland flows to northern Europe, where the soil moisture is reduced. In such situations, very high temperatures are simulated over land. Over the Baltic Sea, the increase in the extreme maximum temperature is more modest, because the high heat capacity and mixing of surface water resist rapid temperature variations.

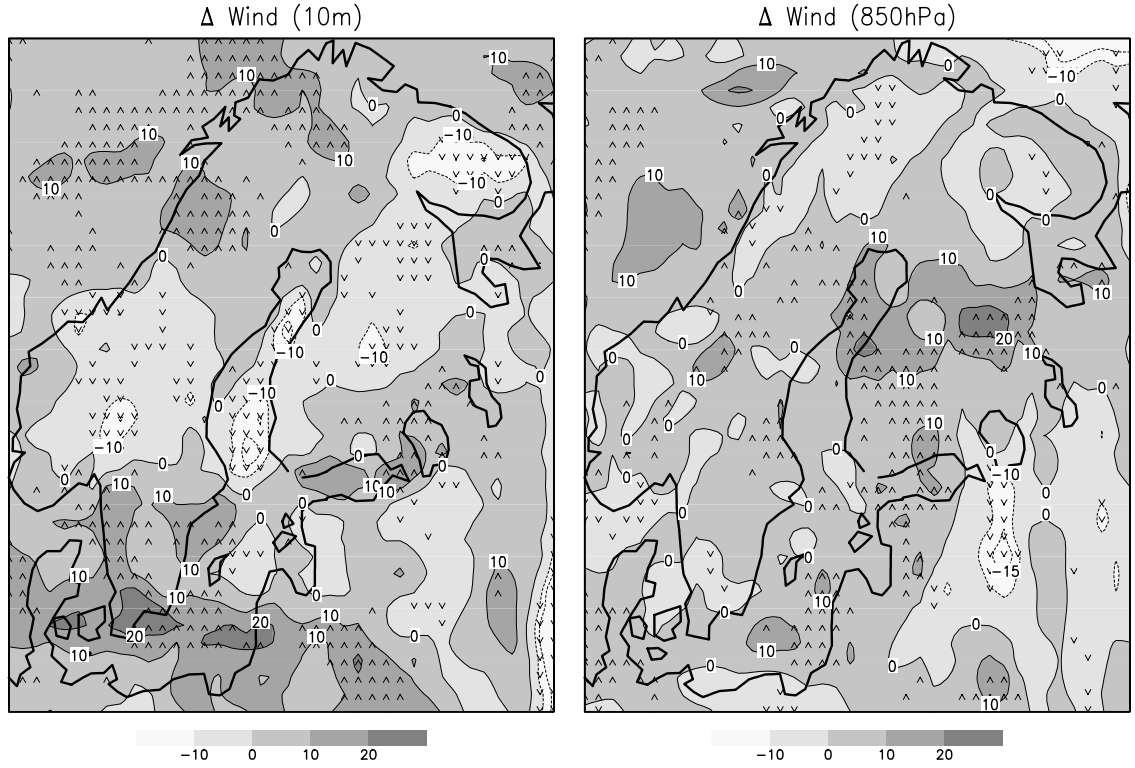

Fig. 5. Same as in Fig. 4 but for the 10-minute mean wind speed at 10 m height (left) and at 850 hPa level (right) in percent.

The results for the changes in the 10-minute mean wind speed at 850 hPa level and at 10 meter height are shown in Fig. 5. These two results appear to be unrelated. This is because the annual extremes of upper air and surface wind speeds are caused by different meteorological events, which may occur in different seasons. This phenomenon is partly related to the high seasonal variations in the stability of the atmospheric boundary layer in the Nordic area.

The simulated changes in the 50-year return values of the precipitation amount in six hours and in five days are shown in Fig. 6. Although the patterns on these maps are noisy, an increase in heavy precipitation is prevalent in both cases. This is consistent with an increase in the atmospheric water vapour in a warmer climate (e.g. *Meehl et al*., 2000). Some of the patterns in Fig. 6 appear to be shaped by the land-sea distribution. Most noticeable of them is the large increase in the six-hour precipitation maxima just off the east coast of Sweden, which appears in some form in all four scenario simulations. However, the physical explanation in this case is not clear. Further studies on the atmospheric processes occurring in this area during different seasons are required.

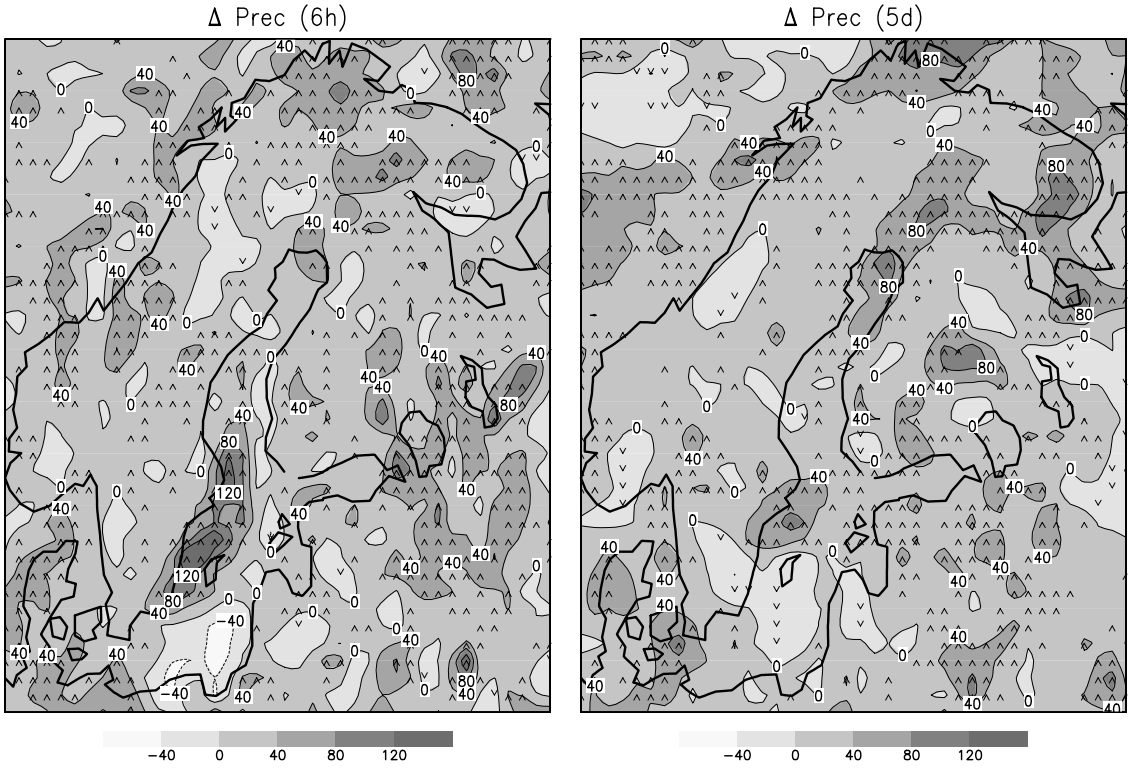

Fig. 6. Same as in Fig. 4 but for the precipitation amount in six hours (left) and in five days (right) in percent.

The simulated change in the 50-year return value of the six hour snow fall is shown in Fig. 7 (left panel). In contrast to a general decrease in the total annual snowfall in the simulated warmer climate, extreme 6-hour snowfall increases in many areas. This is not very surprising since the precipitation amounts increase in general and the

heaviest snowfalls tend to occur in near-zero temperatures rather than in very cold conditions.

The annual maximum snow load in Fig. 7 (right panel), on the other hand, decreases in our simulations in most of the Nordic area, reflecting a general decrease in the total winter snowfall and more frequent melting episodes. In particular, the snowy winters will be shorter so that the cumulative snow amount will decrease. Nevertheless, local increases in the maximum snow load are found in northern Scandinavia, where the present-day climate is colder and most of the increased winter precipitation in the scenario simulations falls as snow. Note, that this behaviour is specific to the 50-year extremes; the average yearly maximum snow load does not increase in any area (*Räisänen et al*., 2003).

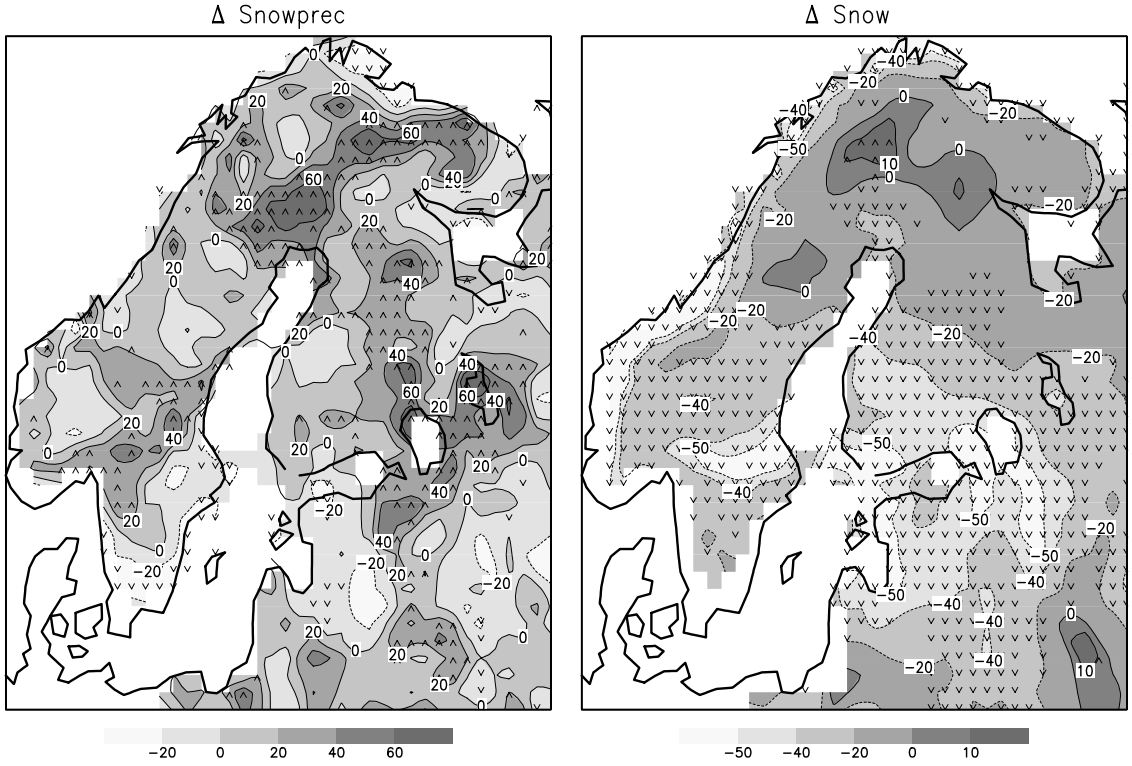

Fig. 7. Same as in Fig. 4 but for the maximum precipitation amount as snow (left) and for the maximum snow water equivalent (right) in percent.

4.2 Regional averages

In Figs. 4–7 results for each grid point averaged over the four simulations are presented. In Table 1, on the other hand, regional results, in which averaging is done for each simulation over all grid points (land areas only), are shown. The results of the mean overall simulations are also given in Table 1. Furthermore, the mean change in the 30 annual extremes and the mean change in the mean variable value are given in Table 1 for comparison.

Table 1. Simulated changes in the 50-year return values as averaged over the land area. Average yearly extremes are based on the 30 annual extremes. In the last column, the time mean climate change is calculated for the annual mean values, except for Tmax (mean for June-July-August) and Tmin (mean for December-January-February).

Variable	50-year extremes					Average yearly extremes	Time mean climate
	REA2	REB2	RHA2	RHB2	Mean	Mean	Mean
Tmax (°C)	5.1	2.8	6.4	3.7	4.5	3.0	2.6
Tmin (°C)	11.2	7.7	9.9	7.7	9.1	10.7	5.5
Wind10 (%)	4.4	5.2	-0.6	0.7	2.4	2.8	2.7
Wind850 (%)	1.0	7.6	-1.7	1.2	2.0	2.5	3.9
Prec6h (%)	32.9	22.5	28.2	18.6	25.6	16.3	15.6
Prec5d (%)	25.3	21.9	30.9	16.3	23.6	11.8	15.6
Snowp6h (%)	17.4	20.2	4.0	8.8	13.0	0.7	-37.4
Snow (%)	-31.8	-21.6	-24.0	-22.5	-24.5	-49.1	-67.2

Although there are differences between the four simulations, they all agree on an increase in the 50-year return value of the maximum and minimum temperature extremes. As expected, the warming is larger for the A2 than the B2 scenario. Area mean changes in the 50-year temperature extremes are similar to the changes in the average yearly extremes discussed by *Räisänen et al*. (2004), although the 50-year maximum temperatures tend to increase slightly more than the average yearly maxima. However, the increase in both the 50-year and average yearly minimum temperatures is almost a factor of two larger than the average wintertime warming.

There is a slight increase in the area mean of the 50-year maximum wind speeds in the two ECHAM4/OPYC3-driven simulations (REA2 and REB2) both at 10-meters and the 850 hPa level, but virtually no change in the HadAM3H-driven simulations (RHA2 and RHB2). This difference, which is similar to that seen in average and yearly maximum wind speeds and the annual mean wind speed (*Räisänen et al*., 2004), relates to the different changes in the large-scale atmospheric circulation in the two global models. While ECHAM4/OPYC3 simulates a northward shift in the North Atlantic storm track and an increase in westerly winds in northern Europe (*Räisänen et al*., 2003, 2004), particularly in winter, such changes are essentially absent in HadAM3H.

The area mean of the 50-year extremes of 6-hour and 5-day precipitation increase in all four simulations. There is no systematic difference in the magnitude of the change between the 6-hour and the 5-day time scales. However, the 50-year extremes tend to increase somewhat more than the average yearly extremes and the mean annual precipitation.

The area mean of the average 6-hour snowfall increases less than the extreme 6-hour precipitation. Nevertheless, the results for the 6-hour snowfall are in clear contrast with the pronounced decrease in the average annual snowfall. Somewhat larger increase

in the 6-hour snowfall is found in REA2 and REB2 than in RHA2 and RHB2, likely because of the increase in wintertime cyclone activity transmitted to RCAO from ECHAM4/OPYC3.

The area mean of the 50-year extreme of maximum snow load decreases substantially in all the simulations. However, there is a systematic north-south difference in the change, which makes such area means somewhat misleading. The average yearly extremes of snow load decrease more than the 50-year maxima. This indicates that snow conditions are, in relative terms, becoming more variable.

5. Discussion

5.1 General remarks

All the simulations analysed in this study indicate a general warming of the 50-year return maximum and minimum temperatures in northern Europe. They also agree on a general increase in the 50-year return value of both the 6-hour and the 5-day precipitation. For extremes of 10-meter wind speed, the results are more variable. The simulations using boundary data from the ECHAM4/OPYC3 model indicate, on the average, an increase of the order of 5%, whereas the simulations with the HadAM3H boundary data show very little area mean change (Table 1). As discussed in Section 4.2, this difference, and perhaps also the larger increases in extreme snowfall in the ECHAM4/OPYC3-driven than in the HadAM3H-driven simulations, reflects different changes in the large-scale atmospheric circulation in the two global models.

Unfortunately no objective quantitative error limits can be given to our climate change predictions of extremes. This is because the global climate modelling errors cannot be readily quantified (*Palmer and Räisänen*, 2002, *Tebaldi et al*., 2005) and because the global emission scenarios A2 and B2 are only a subjectively selected subset of all possible projections. Furthermore, the errors related to the regional model RCAO are still relatively poorly known (*Räisänen et al*., 2004). Nevertheless, the general features of these projections appear realistic. For example, the warming of temperature extremes along with the overall greenhouse-gas induced warming and the increase in extreme precipitation with more water vapour in the atmosphere are both physically plausible and supported by several earlier studies (e.g. *Meehl et al.,* 2000, *Cubasch et al*., 2001, *Kharin and Zwiers*, 2005).

As to the significance of the local patterns in our results, our grid point values include random noise, as discussed in Section 3.2. Thus, in spite of the averaging using four simulation comparisons, some of the local patterns in Figs. 4 to 7 may not represent such changes that would likely appear in the same area in another 30-year run or, more importantly, in connection with the real future climate change. Unfortunately, climate model simulations of this kind are two laborious to be repeated many times in order to detect that way the “real” regional patterns from those caused by spatially random variations. Furthermore, rigorous measures of statistical significance are inapplicable here because we allow the distribution parameters to change freely at each grid point

and in all simulations, so that no specific distribution can be used as a model to estimate the overall errors in the differential values objectively. Bootstrap methods (e.g. *Semmler and Jacob*, 2004) are also inefficient here, because the resulting x^{50} values are very sensitive to the one largest value in a sample. As discussed above, the only effective way around this problem would be to neglect the largest values – a dangerous procedure when making predictions towards an unknown climate.

Another reason for the inapplicability of objective measures of statistical significance here becomes evident from inspection of the exceptional example in Fig. 2, in which the increase in the variable x^{50} from the control run to the prediction run is more than six fold. This very "significant" increase appears, however, to be caused solely by a single biggest extreme (Fig. 2b) that has the lowest statistical confidence. Thus, many of the individual grid point values that are most significant in terms of magnitude are the least significant in terms of statistical confidence.

Due to these difficulties in quantifying error estimates for the grid point values in our overall predictions, we have adopted in Figs. 4 to 7 a rough significance index that is based on the mutual agreement of the four simulation comparisons. In the figures, the grid points at which all the four predictions for the direction of the change agree are marked (ˆ for an increase and ˇ for a decrease), whereas those grid points at which the predictions disagree are unmarked. As expected, the simulation results best agree over wide areas for maximum and minimum temperatures and the snow load.

While there is spatial noise in the figures, many of the regional features seen in our simulation results are physically plausible. Examples include (1) a very significant warming of extreme minimum temperatures over major inland lakes and the Baltic Sea, particularly its southern parts, due to the disappearance of wintertime ice cover; (2) a larger increase in extreme maximum temperatures in the Baltic countries and Finland than over the Baltic Sea, where the heat capacity of the sea and the evaporation from the permanently wet surface resist the increase in summertime temperature extremes; and (3) the small relative decrease (or even local increase) in the extreme snow amount in the northernmost and highest parts of the study area, where the cold present-day climate makes snow conditions relatively less sensitive to the warming. In some other cases as well, the patterns of changes appear to be shaped by the local topography and land-sea distribution, even though the physical explanations are less clear. This emphasizes the importance of a small grid size and taking into account, in the modelling, the local water bodies and other regional geographic details.

As noted in the introduction, there are several earlier model studies on changes in climate variability and extremes in Europe. While differences in methods complicate a detailed comparison, the findings from our simulations (to the extent that our simulations agree with each other) seem to agree qualitatively with these studies. A very large increase in the lowest winter temperatures where snow and ice retreat seems to be a robust feature in other simulations (e.g., *Hegerl et al*., 2004), although a comparison among the PRUDENCE RCMs (*Kjellström et al*., 2007) suggests that RCAO is, in this respect, near the upper end of the range. The smaller but still substantial warming of the highest summer temperatures in Scandinavia is also supported by *Kjellström et al*.

(2007). Similarly, increases in short-term precipitation extremes in northern Europe are a common feature of the PRUDENCE simulations (*Frei et al*., 2006) and a large number of GCM studies (e.g. *Semenov and Bengtsson*, 2002, *Hegerl et al*., 2004, *Kharin and Zwiers*, 2005). However, as noted in the introduction, projections for wind extremes are more variable also among other GCM and RCM studies, although possibly with some predominance of studies that have suggested an increase in wind speeds. To our knowledge, there are no earlier studies on changes in extreme snow depth and snowfall in northern Europe.

When further considering the validity of our modelling results one may investigate how well the control simulations describe the present climate. A general assessment of the simulation of the present-day climate by the RCAO model is provided by *Räisänen et al*. (2003). Such an assessment for the extreme values of interest here is not straightforward and is hampered by the lack of long time-series of homogenous observation data. This will be a subject of a separate study, but we have made tentative comparisons using the available extreme value analysis of observations from some Finnish weather stations (*Makkonen*, 2001, *Venäläinen et al*., 2007). These comparisons show that for the 50-year return values the maximum air temperature is well described by the model results with a small underestimation. The minimum air temperature is simulated well in the coldest parts of the model domain but in coastal areas the models suggest minimum temperatures that are almost 10 °C colder than those based on observations. The extreme surface wind velocity is underestimated by as much as 30%. The extreme maximum 5 day precipitation amount is well simulated with a slight underestimation. The extreme annual maximum snow load is very well simulated.

These tentative results generally support the usefulness of the model simulations for the extremes except, perhaps, in offshore and coastal areas. A systematic error in simulating a present climate variable does not necessarily mean that the change in it is poorly estimated, so that we have presented here the results for the projected change for the whole model domain. Clearly, however, the regional model RCAO, and possibly also the global models, should be improved in their ability to simulate extreme temperatures near the coastline and extreme wind velocities.

5.2 Adaptation needs revealed

As discussed above, the results of our four regional climate change simulations include common features but also differences, in particular in their local details. Since no clear distinction can be made between the qualities of the four scenario runs, it is prudent to view them by averaging their results, as done here. In the following, our results are discussed from the viewpoint of their most important application, i.e. the adaptation requirements in civil engineering practices.

The changes in the extreme maximum and minimum temperatures are large. The average increase over land of the former is about 5 °C and of the latter about 9 °C. The increase in minimum temperatures may not require special adaptation actions, but instead suggests the possibility to reduce the maximum capacity of heating systems in

the future. The increase in the extreme maximum temperatures must, however, be taken into account in designing the maximum capacity of refrigeration systems.

The 50-year return value of the wind speed is one of the most important structural design criteria, particularly for special structures, such as communication towers, suspension bridges and overhead electric power transmission lines. According to our results (Fig. 5, left panel), extreme wind speeds in the Nordic do not seem to increase significantly with climate change. An exception is Denmark, the southern tip of Sweden and parts of the Baltic Sea. The simulated increase in extreme winds in these areas indicates a need to increase the reference wind velocity for the building codes.

The precipitation amount in six hours is a relevant predictor of the likelihood of floods, particularly in urban areas, where most of the drainage occurs via built sewage systems. Our results show a generally increasing trend in this variable. The extremes for a five day cumulative precipitation amount also increase. Overall, the simulated changes in the precipitation extremes are so large that, based on them, large-scale renovation in the drainage capacity is required, particularly in urban areas. In addition, management of the water level of many water reservoirs in the study area should be re-evaluated in view of flooding and dam safety.

The occurrence of heavy snow falls is very important to road maintenance and airport operations. Our analysis (Fig. 7, left) suggests that, despite a widespread decrease in total annual snowfall in a warmer climate, extreme six hour snow precipitation will increase in most parts of the Nordic area. Increasing extreme snow precipitation intensities may initiate more severe snow and ice accretion on structures, such as power lines and communication towers.

The 50-year extreme annual maximum snow water equivalent is important to the design of buildings because it is closely related to the snow loads on roofs. According to our results (Fig. 7, right panel), the extreme snow amount decreases in most of the Nordic area, particularly its southern and western parts, where the simulated future climate includes almost no snow cover at all. Far in the north, however, the decrease is smaller and extreme snow amounts may actually locally increase. These results show that for optimal structural design, the snow load maps of building codes should be updated taking the local differences carefully into account.

Acknowledgements

We thank Dr. M. Rummukainen and the Rossby Centre, Swedish Meteorological and Hydrological Institute for their participation in this project by providing the RCAO data. This work was funded by the Ministry of Environment, Finland.

References

Anon, 2001. CEN.prEN1990 – Eurocode: Basis of Structural Design, European Committee for Standardization, CEN

Beniston, M., D.B. Stephenson, O.B. Christensen, C.A.T. Ferro, C. Frei, S. Goyette, K. Halsnaes, T. Holt, K. Jylhä, B. Koffi, J. Palutikof, R. Schöll, T. Semmler and K. Woth, 2007. Future extreme events in European climate: An exploration of regional climate model projections, *Clim. Change* (in press).

Brabson, B.B. and J.P. Palutikof, 2000. Tests of the generalized Pareto distribution for predicting extreme wind speeds, *J. Appl. Meteorol*., **39**, 1627–1640.

Bringfelt, B., J. Räisänen, S. Gollvik, L.P. Graham and A. Ullerstig, 2001. The land surface treatment for the Rossby Centre regional atmospheric climate model – version 2 (RCA2), *SMHI Reports Meteorology and Climatology*, **98**, Swedish Meteorological and Hydrological Institute, 40 pp.

Castillo, E., 1988. *Extreme Value Theory in Engineering*. Academic Press, New York.

Christensen, J.H., T.R. Carter and M. Rummukainen, 2007. Evaluating the performance and utility of regional climate models: the PRUDENCE project. *Clim. Change* (in press).

Coles, S., 2001. *An Introduction to Statistical Modeling of Extreme Values*. Springer, London.

Cook, N.J., 1982. Towards better estimation of extreme winds. *J. Wind Eng. Ind. Aerodyn.*, **9**, 295–323.

Cook, N.J., R.I. Harris and R. Whiting, 2003. Extreme wind speeds in mixed climates revisited. *J. Wind Eng. Ind. Aerodyn*., **91**, 403–422.

Cubasch, U., G.A. Meehl, G.J. Boer, R.J. Stouffer, M. Dix, A. Noda, C.A. Senior, S. Raper and K.S. Yap, 2001. Projections of future climate change. In: *Climate Chang*e. Cambridge University Press, p. 525–582.

Cunnane, C., 1978. Unbiased plotting positions – a review. *J. Hydrol*., **37**, 205–222.

Döscher, R., U. Willén, C. Jones, A. Rutgersson, H.E.M. Meier and U. Hansson, 2002. The development of the coupled ocean-atmosphere model RCAO. *Boreal Env. Res*., **7**, 183–192.

Eerola, K., D. Salmond, N. Gustafsson, J.A. Garcia-Moya, P. Lönnberg and S. Järvenoja, 1997. A parallel version of the HIRLAM forecast model: strategy and results. Proc. 7th ECMWF Workshop on the use of parallel processors in meteorology. *World Sci. Publ*., p. 134–143.

Ekström, M., H.J. Fowler, C.G. Kilsby and P.D. Jones, 2005. New estimates of future changes in extreme rainfall across the UK using regional climate model integrations. 2 Future estimates and use in impact studies, *J. Hydrol*., **300**, 234–251.

Fisher, R.A. and L.H.C. Tippett, 1928. Limiting forms of the frequency distributions of the largest or smallest members of a sample. *Proc. Cambridge Phil. Soc*., **24**, 180–190.

Folland, C. and C. Anderson, 2002. Estimating changing extremes using empirical ranking methods, *J. Clim*., **15**, 2954–2960.

Frei, C., R. Schöll, S. Fukutome, J. Schmidli and P.L. Vidale, 2006. Future change of precipitation extremes in Europe: Intercomparison of scenarios from regional climate models, *J. Geophys. Res*. 111, D06105, doi:10.1029/2005JD005965.

Galambos, J. and N. Macri, 1999. Classical extreme value model and prediction of extreme winds, *J. Structural. Eng*., **125**, 792–794.

Gomes, L. and B.J. Vickery, 1978. Extreme wind speeds in mixed climates, *J. Wind Eng. Ind. Aerodyn*., **2**, 331–344.

Gordon, C., C. Cooper, C.A. Senior, H. Banks, J.M. Gregory, T.C. Johns, J.F.B. Mitchell and R.A. Wood, 2000. The simulation of SST, sea ice extent and ocean heat transport in a version of the Hadley Centre coupled model without flux adjustments, *Clim. Dyn*., **16**, 147–166.

Gringorten, I.I., 1963. A plotting rule for extreme probability paper, *J. Geophys. Res*., **68**, 813–814.

Gumbel, E.J., 1958. *Statistics of Extremes*. Columbia University Press, New York.

Harris, R.I., 1996. Gumbel re-visited – a new look at extreme value statistics applied to wind speeds, *J. Wind Eng. Ind. Aerodyn*., **59**, 1–22.

Harris, R.I., 1999. Improvements to the "Method of independent Storms", *J. Wind Eng. Ind. Aerodyn*., **80**, 1–30.

Harris, R.I., 2000. Control curves for extreme value methods, *J. Wind Eng. Ind. Aerodyn.*, **88**, 119–131.

Harris, R.I., 2004. Extreme value analysis of eoch maxima – convergence, and choise of asymptote, *J. Wind Eng. Ind. Aerodyn*., **92**, 897–918.

Hazen, A., 1914. Storage to be provided in impounding reservoir for municipal water supply, *Trans. Amer. Soc. Civ. Eng*., **77**, 1547–1550.

Hegerl, G.C., F.W. Zwiers, P.A. Stott and V.V. Kharin, 2004. Detectability of anthropogenic changes in annual temperature and precipitation extremes, *J. Clim*., **17**, 3683–3700.

Hosking, J.R., 1985. Maximum-likelihood estimation of the parameters of the generalized extreme-value distribution, *Appl. Stat*., **34**, 301–310.

Hosking, J.R., J.R. Wallis and E.F. Wood, 1985. Estimation of the generalized extreme value distribution by a method of probability weighted moments. *Technometrics*, **27**, 251–261.

Huntingford, C., R.G. Jones, C. Prudhomme, R. Lamb, J.H.C. Gash and D.A. Jones, 2003. Regional climate-model predictions of extreme rainfall for a changing climate, *Quart. J. R. Meteor. Soc*., **129**, 1607–1621.

Jones, C.G., U. Willén, A. Ullerstig and U. Hansson, 2004. The Rossby Centre Regional Atmospheric Climate Model, Part I: Model climatology and performance for the present climate over Europe, *Ambio*, **33**, 199–210.

Jordaan, I., 2005. Decisions under Uncertainty. Cambridge University Press, 672 pp.

Jylhä, K., H. Tuomenvirta and K. Ruosteenoja, 2004. Climate change projections for Finland during the 21st century, *Boreal Env. Res*., **9**, 127–152.

Katz, R.W., M.B. Parlange and P. Naveau, 2002. Statistics of extremes in hydrology, *Adv. Water Resour.*, **25**, 1287–1304.

Kharin, V.V. and F.W. Zwiers, 2005. Estimating extremes in transient climate change simulations, *J. Clim*., **18**, 1156–1173.

Kjellström, E., L. Bärring, D. Jacob, R. Jones, G. Lenderink and C. Schär, 2007. Variability in daily maximum and minimum temperatures: recent and future changes over Europe, *Clim. Change* (in press).

Landwehr, J.M., N.C. Matalas and J.R. Wallis, 1979. Probability weighed moments compared with some traditional techniques in estimating Gumbel parameters and quantiles, *Water Resour. Res*., **15**, 1055–1064.

Leckebusch, G.C. and U. Ulbrich, 2004. On the relationship between cyclones and extreme windstorm events over Europe under climate change, *Global Planet. Change*, **44**, 181–193.

Lieblein, J., 1974. Efficient methods of extreme-value methodology, *National Bureau of Standards (U.S.)*, Report **NBSIR 74-602**.

Makkonen, L., 2001. CEN esistandardin Eurocode 1 "Actions on Structures", Part 1.4: General Actions – Wind Actions liittyvän tuulennopeuden perusarvon (reference wind velocity) päivitys Suomen osalta. VTT Tutkimusselostus NRO **RTE4627/01**, Technical Research Centre of Finland, VTT, 6 pp.

Makkonen, L., 2006. Plotting positions in extreme value analysis, *J. Appl. Meteorol. Climatol*., **45**, 334–340.

Makkonen, L. 2007. Problems in the extreme value analysis, *Structural Safety* (in press).

Makkonen, L. 2008. Bringing closure to the plotting position controversy. *Commun. Stat.–Theory Methods*, **37** (in press).

Martins, E.S., Stedinger, J.R., 2000. Generalized maximum likelihood generalized extreme-value quantile estimators for hydrological data, *Water Resour. Res*., **36**, 737–744.

Meehl, G.A., Zwiers, F.W., Evans, J., Knutson, T., Mearns, L., Whetton, P., 2000. Trends in extreme weather and climate events: Issues related to modeling extremes in projection of future climate change, *Bull. Amer. Meteor. Soc*., **81**, 427–436.

Meier, H.E.M., 2001. On the parameterization of mixing in 3D Baltic Sea models, *J. Geophys. Res*., **106**, 30997–31016.

Meier, H.E.M., Döscher, R., Coward, A.C., Nycander, J., Döös, K., 1999. Rossby Centre regional ocean climate model: model description (version 1.0) and first results from the hindcast period 1992/1993, *SMHI Reports Oceanography* **26**, Swedish Meteorological and Hydrological Institute, Norrköping, Sweden, 102 pp.

Nakićenović, N., Alcamo, J., Davis, G., de Vries, B., Fenhann, J., Gaffin, S., Gregory, K., Grubler, A., Jung, T.Y., Kram, T., La Rovere, E.L., Michaelis, L., Mori, S., Morita, T., Pepper, W., Pitcher, H., Price, L., Raihi, K., Roehrl, A., Rogner, H-H., Sankovski, A., Schlesinger, M., Shukla, P., Smith, S., Swart, R., van Rooijen, S., Victor, N., Dadi, Z., 2000. Emission Scenarios. A Special Report of Working Group III of the Intergovernmental Panel on Climate Change, IPCC, Cambridge University Press, 599 pp.

Pall, P., Allen, M.R., Stone, D.A., 2007. Testing the Clausius-Clapeyron constraint of changes in extreme precipitation under CO2 warming, *Clim. Dyn*., **28**, 351–363.

Palmer, T.N., Räisänen, J., 2002. Quantifying the risk of extreme seasonal precipitation events in a changing climate, *Nature*, **415**, 512–514.

Peterka, J.A., 1992. Improved extreme wind prediction for the United States, *J. Wind Eng. Ind. Aerodyn*., **41–44**, 533–541.

Pickands, J., 1975. Statistical interference using extreme order statistics, *Ann. Stat*., **3**, 119–130.

Pryor, S.C., Barthelmie, R.J., Kjellström, E., 2005a. Potential climate change impact on wind energy resources in northern Europe: Analyses using a regional climate model, *Clim. Dyn*., **25**, 815–835.

Pryor, S.C., School, J.T., Barthelmie, R.J., 2005b. Potential climate change impacts on wind speeds and wind energy density in northern Europe: Results from empirical downscaling of multiple AOGCMs, *Climate Res*., **29**, 183–198.

Räisänen, J., 2001. The impact of increasing carbon dioxide on the climate of northern Europe in global climate models (in Finnish with English abstract and figure and table captions), *Terra*, **113**, 139–151.

Räisänen, J., Hansson, U., Ullerstig, A., Döscher, R., Graham, L.P., Jones, C., Meier, M., Samuelsson, P., Willén, U., 2003. GCM driven simulations of recent and future climate with the Rossby Centre coupled atmosphere – Baltic Sea regional climate model RCAO. *SMHI Reports Meteorology and Climatology*, No. **101**, Swedish Meteorological and Hydrological Institute, 61 pp.

Räisänen, J., Hansson, U., Ullerstig, A., Döscher, R., Graham, L.P., Jones, C., Meier, M., Samuelsson, P., Willén, U., 2004. European climate in the late 21st century: regional simulations with two driving global models and two forcing scenarios, *Clim. Dyn*., **22**, 13–31.

Rasmussen, P.F., Gautam, N., 2003. Alternative PMW-estimators of the Gumbel distribution, *J. Hydrol*., **280**, 265–271.

Rockel, B., Woth, K., 2007. Future changes in near surface wind speed extremes over Europe from an ensemble of RCM simulations, *Clim. Change* (in press).

Roeckner, E., Bengtsson, L., Feichter, J., Lelieved, J., Rodhe, H., 1999. Transient climate change simulations with a coupled atmosphere-ocean GCM including the tropospheric sulfur cycle, *J. Clim*., **12**, 3004–3032.

Schär, C., Vidale, P.L., Lüthi, D., Frei, C., Häberli, C., Liniger, M.A., Appenzeller, H., 2004. The role of increasing temperature variability in European summer heatwaves, *Nature*, **427**, 332–336.

Semenov, V.A., Bengtsson, L., 2002. Secular trends in daily precipitation characteristics: greenhouse gas simulation with a coupled AOGCM, *Clim. Dyn*., **19**, 123–140.

Semmler, T., Jacob, D., 2004. Modeling extreme precipitation events – a climate change simulation for Europe, *Global Planet. Change*, **44**, 119–127.

Simiu, E., Heckert, N.A., 1996. Extreme wind distribution tails: A "Peak over threshold approach", *J. Struct. Eng*., **122**, 539–547.

Solomon, S., Qin, D., Manning, M., Chen, Z., Marquis, M., Averyt, K.B., Tignor, M., Miller, H.L. (eds.), 2007. Climate Change 2007: The Physical Science Basis. Contribution of Working Group I to the Fourth Assessment Report of the Intergovernmental Panel of Climate Change, IPCC, Cambridge Univ. Press, 996 pp.

Tebaldi, C., Smith, R.L., Nychka, D., Mearns, L.O., 2005. Quantifying uncertainty in projections of regional climate change A Bayesian approach to the analysis of multimodel ensembles, *J. Clim*., **18**, 1524–1540.

Venäläinen, A., Saku, S., Kilpeläinen, T., Jylhä, K., Tuomenvirta, H., Vajda, A., Ruosteenoja, K., Räisänen, J., 2007. Sään ääri-ilmiöistä Suomessa. Ilmatieteen laitos, Raportteja, No. **2007:4**, Finnish Meteorological Institute, 81 pp. (in Finnish)

Wang, Q.J., 1991. The POT model described by the generalized Pareto distribution with Poisson arrival rate, *J. Hydrol*., **129**, 263–280.